

Renewable Energy Research and Applications (RERA)



Vol. 6, No. 2, 2025, 269-283 10.22044/rera.2023.12548.1191 DOI:

An Experimental Study to Evaluate Performance of an HDH Water Desalination System with a Thermoelectric Condenser

M. Rezaei Rad, R. Shafaghat*, A. H. Aghajani Afghan and B. Alizadeh Kharkeshi

Babol Noshirvani University of Technology, Sea-Based Energy Research Group, Babol, Iran.

Received Date 24 December 2024; Revised Date 10 March 2025; Accepted Date 11 March 2025 *Corresponding author: rshafaghat@nit.ac.ir (R. Shafaghat)

Abstract

This experimental study introduces a solar humidifier-dehumidifier desalination model as a type of open-air-open water (OAOW) system; also, a new condenser with thermoelectric modules is applied in dehumidifier unit. The experimental tests are done by considering climate conditions in the north of Iran (Mazandaran province, Babol), and the effect of the inlet air's temperature and flow rate on the system's functional characteristics and condenser is investigated to improve the performance. Sensors measuring the data are related to the fluid temperature and humidity of the cycle at different points; other data is also gathered by psychrometric chart and EES software. The results section investigates the water generation rate, GOR, coefficient of performance (COP), and condenser efficiency. The results show that the highest water production is 420 g/hr, and the highest GOR is 0.19. Also the water production rate and COP increase as the inlet air temperature rises. At temperatures lower than 75 °C, due to the air saturation, the maximum point of the water production, and COP occurs at a flow rate of 0.022 kg/s. At high temperatures, increasing the flow rate raises water production, and on the other hand, the COP in the condenser is 0.8 at the highest point. According to the economic analysis done for the proposed model, the freshwater cost is 0.098-0.049 \$/year for one liter.

Keywords: Solar Water Desalination, HDH Water Desalination, Thermoelectric Cooling Module, Thermoelectric Condenser.

1. Introduction

The water crisis is considered as one of this century's main challenges, which will cause many positive and negative effects in the world. Various factors such as population growth, industrial development, and the expansion of agriculture have caused a significant increase in water consumption in different countries. As predicted, worldwide water resources will be 40% less than the global water demand by 2030 [1]. Today, desalination is usually used to overcome the lack of fresh water in some regions where brine or brackish water is available. In order to achieve fresh water, various technologies have been developed. Most of the available technologies are reverse osmosis (RO), multi-stage distillation (MSF), and multi-effect distillation (MED), which have a water production capacity of more than 100 m³/hr. Also these technologies require much energy to start up, and are usually built next to power plants. To provide fresh water, variables such as the economic efficiency of the water desalination system, maintenance costs, and

the type of available energy should be considered. Considering the capacity of most regions suffering from a freshwater crisis, only solar energy can satisfy all the above conditions. In conventional technologies, high energy costs are spent on increasing the temperature due to the high working temperature. However, the state of the art humidifier-dehumidifier (HDH) desalination system is placed in the category of direct water desalination, and operates with low temperature for a start-up due to low thermal energy consumption. These water desalination systems can be run on solar energy. The HDH process is based on the fact that air can carry large amounts of water vapor. The ability to carry water growths with increasing by air temperatures. Theoretically, 1 kg of dry air can carry 0.5 kg of water vapor with energy consumption of 2814 kJ and an increase in temperature from 30 °C to 80 °C [2]. Also this type of water desalination system is attractive to most researchers in this field due to its advantages such as small-scale installation, simple design, flexibility, low maintenance and investment costs, and the ability to start using waste heat or renewable energy sources [3]. The HDH process can be classified into three divisions: energy consumption, cycle, and heating system. Based on the energy consumption concept, HDH systems classified into three categories: solar, geothermal, and hybrid [2]. Notably, most reported HDH desalination systems utilize solar energy [3]. Many researchers have investigated the relationship between freshwater production rate and solar radiation intensity for HDH systems. Deniz et al. [4] showed the relationship between solar radiation and water production during the day. According to their study, the amount of freshwater produced in HDH systems is directly related to the radiation intensity. Alam et al. [5] presented different heat transfer techniques to enhance the performance of doublepass solar air heaters (SAHs). The results showed that the heat transfer from the absorber plate to the air could be improved by increasing the convection heat transfer coefficient and the heat transfer area and reducing the heat loss. In this experimental study, it was shown that double-pass SAHs perform better than single-pass SAHs.

The division of the HDH system is described based on the seawater and air cycle, which can be closed or opened [6]. In general, there are three different configure rations of HDH systems such as closed air-open water (CAOW), open air-open water (OAOW), and open air-closed water (OACW) cycles. In addition, HDH systems are divided into two categories, water heating (WH) and air heating (AH) based on the type of fluid heating [7]. Different HDH cycles for integration with solar air heaters or solar water heaters are shown in figure 1.

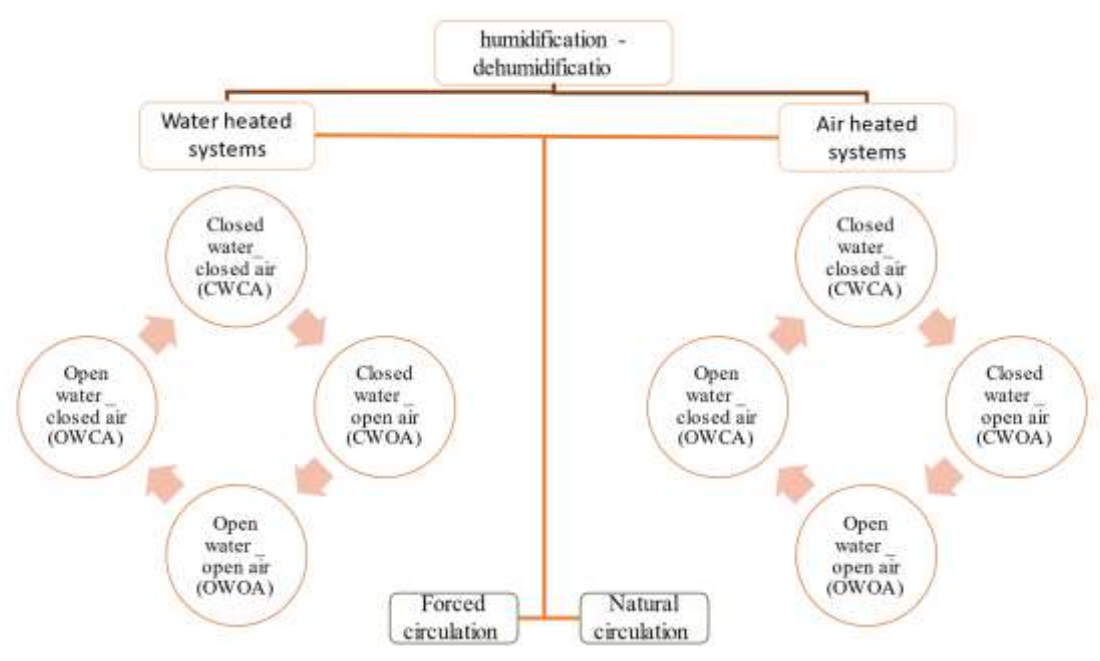


Figure 1. Different types of HDH system cycles.

According to the reviews of Alexander *et al.* [8], the OAOW-WH cycle is independent from the environment's relative humidity, and they always perform better compared to the CAOW-WH cycle. They also showed that the CAOW-AH cycle was usually more efficient than the OAOW-AH cycle, except when the relative humidity of the environment was close to 100%. Therefore, it can be said that "In the humid regions of the world, due to the inherent high air humidity, openair cycles have a better performance." Also Sharqawy *et al.* [9] to compare the GOR in HDH systems, reported that air-heating and waterheating HDH cycles have almost the same GOR.

Most systems studied in this type of water desalination system are designed as open water. In HDH systems, for dehumidification in the dehumidifier section, low-temperature salt water is used as a coolant in the condensing tubes [10]. One disadvantage of the closed water system is the increased water temperature during the cycle. This weakness is a significant concern in systems whose condenser must be cooled by water, while the open water system does not have this problem. In places where brine water is abundant, it is better to use an open water system. Extensive research was conducted on solar **HDH** desalination plants. Yasser Elhanavi et al. [11]

conducted a theoretical study on a solar HDH desalination plant to investigate the effect of weather conditions on efficiency. The designed set consisted of solar water and an air collector to provide hot water and air for the system. The system was divided into two groups: humidifying and dehumidifying towers. The heat and mass balance was applied, and a set of governing equations were solved using the finite difference method, and finally, the average accumulated production rate of the system in winter was between 2.5 and 4 (kg/m²)/day, while the average summer production rate was between 8 and 12 (kg/m²)/day.

As an emerging technology, thermoelectric cooling and heating modules have attracted the researchers' attention in the recent years. Thermoelectric modules have no sound and vibration, have an extended life, and have lightweight; they are also environmentally friendly. In addition, they can work with DC voltage and feed directly from solar cells[12]. Various designs have been presented for their use in air condensers and moisture absorbers. Vian et al. [13] designed the humidifier prototype based on the thermoelectric cooling technology. They concluded that thermoelectric had a significant potential in this field. Yao et al. [14] worked on small dehumidifiers, usually used to reduce the relative humidity inside the building and create comfortable conditions. They experimentally investigated the effect of structural parameters and operating conditions on the dehumidification rate of TED. This study investigated the effect of thermoelectric modules (TEM) arrangement, air channel size, heat sink size, and number of TEMs. The proposed sample provided enough cooling capacity for dehumidification with two heat sinks on the cold side and two heat sinks on the hot side. They concluded that the dehumidification rate of this sample when the air duct flow rate was 1.74 m/s was 33.1 g/hr and the COP was 0.75. In addition, the new configuration significantly improved the dehumidification rate compared to the conventional configuration. In Omedi et al. [15] study, a new HDH system consisting of a hybrid solar collector with two active fluids of air and ethylene glycol was designed and tested under the climatic conditions of Tehran (Iran). In this design, the air passes over the absorber plate while ethylene glycol flows through the copper pipes located in the absorber plate. The dehumidifier system was also equipped with thermoelectric cooling modules. parameters such as collector outlet air velocity, the volume flow rate of ethylene glycol and salt

water, and the effect of thermoelectric cooling on system performance and exergy were investigated. The experimental results showed that water production improved by 8% by increasing the air velocity of the collector outlet from 2.2 to 3 m/s; while increasing the collector outlet air velocity in the range of 3-2.4 m/s, it decreases by 17%. In addition, by increasing the volumetric flow rate of salt water from 0.66 liters per minute to 3 liters per minute, the daily productivity of the system improves by about 55%. Finally, the maximum hourly and daily exergy efficiency were obtained at 12.75% and 8.78%, respectively. Nazari et al. [16] in an experimental study, investigated the performance of copper oxide (Cu₂O) nanofluid in a single-slope solar still that was integrated with a thermoelectric glass cover cooling channel. The results showed that the modified solar stationary device's productivity, energy, and efficiency increased compared to the conventional solar stationary device. In addition, by adding copper oxide nanoparticles to salt water, the productivity, energy, and exergy efficiency increased significantly.

The present study used a thermoelectric condenser to condense and produce water in a solar humidification-dehumidification desalination system as an open-air-open water type. The ambient air is first heated in the air heater, and then humidified by passing through the humidifier. In the last step, hot and humid air will enter the condensing chamber. In the condenser, condensation and distillation are performed by passing humid air through the heat sinks connected to the thermoelectric. In this system, the salt-water flow that enters the humidifier tower is first used to cool the thermoelectric modules, which will pre-heat and increase the efficiency of the humidifier tower and the GOR. In thermoelectric densifications, cooling the hot side is very important for increasing the efficiency of thermoelectricity. In this system, cooling is done by the incoming water to the system, which is better cooled due to the high heat transfer coefficient of water. This has been less studied. Also by absorbing the rejected heat, the temperature of the incoming water increases, which provides a better reason for its evaporation. The cost of water production is one of the important parameters for water production. The cost of water production includes costs related to maintenance, construction, and consumption. Also this system is very simple and designed with low cost. On the other hand, the designed condenser has no moving mechanical parts, noiseless, has a long life, and can be connected to photovoltaic collectors.

The following model of the HDH desalination system combined with the thermoelectric condenser will be introduced as a novel structure for recovering systems waste heat, and then the experimental tests will be described. The results section presents the system's performance in the form of freshwater production rate, thermoelectric condenser performance coefficient, GOR rate, and economic analysis.

2. Experimental study

2. Experimental setup description

The studied system is an HDH active solar water desalination system as the OWOA type. The proposed model consists of three sections: solar air heater, humidifying tower, and condenser (Figure 2). The air first enters the solar air heater, and then hot and dry air is blown into the humidifier tower from the bottom. Brine water is sprayed from the top of the humidifier tower with

a constant flow on the cellulose pad. Hot air is in direct contact with brine water particles, and turns some of them into steam. Thus at the outlet of the humidifier tower, the relative humidity of the air reaches 95%. Next, the air exits from the top of the humidifier tower and enters the condenser. Excess water is also removed from the bottom of the humidifier tower.

The condenser consists of 12 thermoelectrics of TEC1-12706 type, which are regularly placed on the four faces of an aluminum profile with dimensions of 40 × 60 mm and 80 cm long. On the cool surface of thermoelectric, aluminum heat sinks with dimensions of 10 × 5.2 × 5 cm were placed to expand the cool surface (Figure 3). Modules and heatsinks were installed on the aluminum profile using Thermal Paste, and plastic clamps were used to keep them fixed. Finally, the whole collection was placed in a polyethylene tube with a diameter of 15 cm. The dimensions and sizes of all system components are given in table 2.

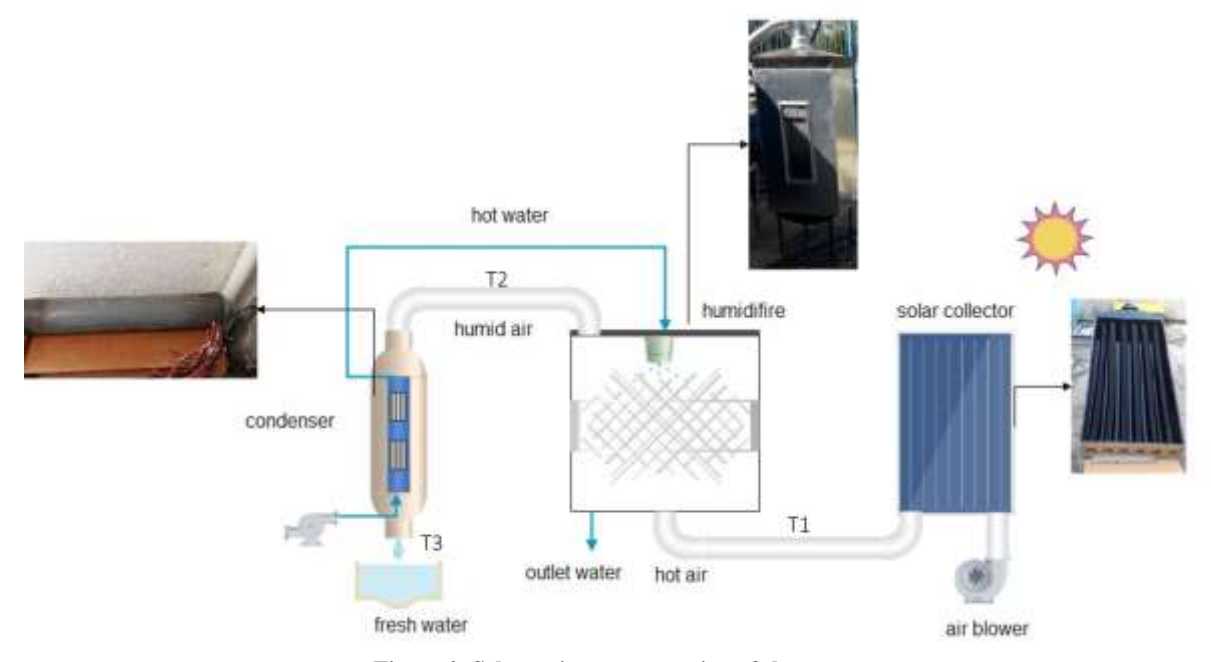


Figure 2. Schematic representation of the system.



Figure 3. Thermoelectric location on the aluminum profile (condenser core).

By connecting to the power source, thermoelectric act like a heat pump, one side of these modules is cold and the other side is heated. To increase the thermal efficiency of the modules, it is necessary to reduce the temperature difference between the two sides. For this purpose, the flow of brine water entering the system was used. As the water flow passes through the aluminum profile, the heat is transferred from the hot surface of the modules to the water, cooling is done, and the temperature of the heat sinks also decreases. Therefore, the salt water entering the humidifier tower is pre-heated. In this research work, the condenser was placed vertically so that the droplets formed on heatsinks due to the weight

force and airflow slide down and are separated from the surface of the heat sinks faster so that the thermal resistance of the surface of the heat sinks is reduced.

Table 1. Parameters and properties of TEC1-12706.

Parameter (unit)	Value
Couples (N)	127
Voltage U _{max} (V)	15.2
Current I _{max} (A)	6
Maximum cooling capacity Qmax (W)	56.5
Maximum temperature difference between	68
hot-side and cold-side ΔT_{max} (°C)	06
Reference temperature at hot side $T_h(^{\circ}C)$	27
Dimensions (mm)	$40 (L) \times 40 (W) \times 3.9 (H)$

Table 2. Specifications of system components.

Components	Specifications
Humidifier tower	650 × 850 mm rectangular cross-section and 2000 mm height, the body material is galvanized sheet, insulated from the inside by Unolite and the outside by glass fibers
Thermoelectric condenser core	Maximum cooling power 678 watts, input power 720 watts
Dehumidifier	Polyethylene pipe with a diameter of 160 mm and a path length of 800 mm and the condensing core was placed inside it vertically
Electric air heater	Maximum power is 3500 watts and the maximum air flow rate is $0.07 \ kg/s$
Air channel	Channel made of galvanized sheet with a circular cross-section with a diameter of 100 mm, insulated by glass .wool

2.2. Measuring equipment

Essential parameters to evaluate the HDH water desalination system's performance include dry bulb temperature of the inlet and outlet air from the humidifier and condenser; the water temperature at the inlet and outlet from the humidifier tower and the dehumidifier were measured by k-type thermocouples and were used together with an ATMEGA32 micro-controller. In

addition, mass flow rates for air and water were also important, so that the water flow rate was calculated experimentally after determining the filling time of a standard container with a stopwatch, and air velocity was founded by using an anemometer. The accuracy of the measurement and the model of the measurement equipment are presented in table 3.

Table 3. Introduction of measuring equipment [17].

Instrument	Resolution	Measurement accuracy	Image
Velocity meter (GM816A)	0.1(m/s)	±5%	
Temperature and humidity sensor (AM1001)	0.1(°C) for Temperature 3% for humidity	±5%	The state of the s

2.3. Uncertainly analysis

Any quantitative measurement is associated with a degree of uncertainty due to various errors in measuring instruments, devices, and tester errors. This research work tried to minimize the errors by applying and observing some methods such as insulating the system and conducting the

experiment in a closed environment the room. Equations (1) to (4) have been used for uncertainty analysis. The results for a sample at inlet air temperature and flow rate equal to 49 degrees Celsius and 0.016 kg/s, respectively, are presented in table 4 [18].

 \overline{x} is the average value of the data, x is the parameter considered in each test, n is the number of tests, s is the standard deviation, u is the uncertainty, and U is the combined uncertainty with the coverage factor k. According to table 4, the reliability of the experimental data is 95% [19, 20]

$$\overline{X} = \frac{\sum_{I=1}^{N} X_{I}}{N} \tag{1}$$

$$S = \sqrt{\frac{\sum_{i=1}^{N} (X_i - X)^2}{(N-1)}}$$
 (2)

$$U = \frac{S}{\sqrt{N}} \tag{3}$$

$$U = KU \tag{4}$$

Table 4. Uncertainty analysis results.

Parameter	1	2	3	4	5	Average	Standard deviation	U	U _c
Dehumidifier outlet temperature	21.7	21.6	21.5	21.4	21.8	21.6	0.15	0.07	0.14
Airflow speed at the dehumidifier outlet	1.7	1.8	1.7	1.6	1.7	1.7	0.071	0.032	0.063

2.4. Test condition

All experiments have been done in Iran, Mazandaran province, and Babol city (latitude: 36.54 N, longitude: 52.68 E, and altitude: -2 m above sea level) in the time intervals between 8 am and 5 pm in March 2022. The test times were performed for the system's three inlet air flow rates equal to 0.016, 0.022, and 0.027 kg/s and four different inlet air temperatures to the humidifier tower (Table 5). In each experiment, the air temperature in the inlet and outlet sections of the air heater, humidifier tower, condenser, and the airflow rate in the condenser, along with the ambient temperature, were recorded. The system components were placed inside the room to reduce measurement error, and rock wool was used to insulate the equipment. It was also tried to keep the room temperature constant. Solar radiation and atmospheric disturbances such as wind do not affect the test data, and the conditions are under better control. For this purpose, in this research work, an electric air heater equivalent to a solar air heater with variable power was used to heat the air; experimental tests were conducted on the solar air heater during the summer season and desired weather conditions. temperature settings of the air outlet from the electric air heater were applied according to the results of this test to match the electric air heater with the solar air heater. Some parameters such as ambient temperature, the flow rate of brine water entering the condenser, and humidifier tower, electrical power entering the thermoelectric, and the power consumption of the pump and blower, were considered constant (Table 6).

To perform the test, first, the air inlet velocity is set by the variable fan. Then the thermal power of the electric heater is gradually increased until the inlet air temperature reaches the desired temperature. Then one hour is given to the system to get a steady state; after that, the test data is

recorded. This process was repeated for two other air speeds and three heat powers.

Table 5. Constant values during the experiment.

Quantity	Unit	Value
Environment temperature	°C	20
Electric power consumption of thermoelectric	W	720
Pump power	W	65
Blower power	W	36
Inlet water flow rate to the humidifier	$^{kg}/_{s}$	0.014

3. Theoretical considerations

After measuring the experimental results, the functional parameters of the water desalination system were calculated by applying the conservation of mass and energy law. Laws of conservation of mass and energy were considered for each component of the system. The airflow rate (\dot{m}_a) was assumed to be constant during the cycle. In the following, the used thermodynamic equations are introduced. The thermal power input to the air in the solar air heater is calculated using equation (5).

$$\dot{Q}_{\text{collector}} = \dot{M}_{\text{A}} C_{p_{air}} (T_{\text{I,H}} - T_{\infty})$$
 (5)

Condenser efficiency (η_{DH}) is also obtained using equation (6).

$$H_{DH} = \frac{\left(\Omega_{I,DH} - \Omega_{O,DH}\right)}{\left(\Omega_{I,DH} - \Omega_{O,DH,S}\right)}$$
(6)

 $\omega_{o,dh,s}$ is absolute humidity, and it is related to the time when the air leaving the dehumidifier in saturated state. The following equation was used to analyze the coefficient of performance of the condenser (COP):

$$\begin{array}{l} \text{COP=} \\ \underline{\text{CP}_{AIR} \times \dot{\text{M}}_{\text{A}}(\text{T}_2 - \text{T}_3) + (\text{H}_{\text{FG}} \times \dot{\text{M}}_{\text{F}}) + (\text{H}_{\text{F2}} \times \omega_2 \times \dot{\text{M}}_{\text{A}}) - (\text{H}_{\text{F3}} \times \omega_3 \times \dot{\text{M}}_{\text{A}})} \\ \underline{\text{E}_{\text{T}}} \end{array} \tag{7}$$

Specific heat capacity of $airCp_{air}$, inlet dry air flow rate \dot{m}_a , enthalpy of the mixture of water and

water vapor h_{fg} , the amount of water produced \dot{m}_f , enthalpy of saturated water at the inlet of the condenser h_{f2} , relative humidity at the inlet of the condenser ω_2 , enthalpy of saturated water at the outlet of the condenser h_{f3} , relative humidity at the outlet of the condenser ω_3 and E_t is the amount of electrical energy given to the condenser. it is calculated from the following equation:

$$E_{T} = E_{TH} + E_{P} \tag{8}$$

 $E_{\rm th}$ is electric energy consumption by thermoelectric and E_p is electric energy consumption by the pump. \dot{m}_a is obtained as follows:

$$\dot{\mathbf{M}}_a = \mathbf{V}_{AIR} \times \mathbf{P} \times \mathbf{A} \tag{9}$$

 ρ is the air density, which was assumed to be a constant number of 1.225 in the calculations. The total thermal efficiency of the system (GOR) is calculated from the following relationship:

$$GOR = \frac{h_{fg} \times \dot{m}_f}{Q_{tot}}$$
 (10)

 Q_{tot} is the total energy supplied to the system. In the calculation of the total heat transfer, the amount of electrical energy consumed by the pump and the thermoelectric modules was taken into account, and a constant value of 720 watts was considered. The amount of theoretically produced water $(\dot{\mathbf{m}}_{ff})$ is calculated from the following equation:

$$\dot{\mathbf{m}}_{ff} = \dot{\mathbf{m}}_a(\omega_2 - \omega_3) \tag{11}$$

 ω_2 and ω_3 are the relative humidity at the inlet and outlet of the condenser, respectively. The difference between experimentally produced water and theoretically produced water is calculated as follows:

$$erorr = \dot{\mathbf{m}}_{ff} - \dot{\mathbf{m}}_f \tag{12}$$

In economic analysis, the following relationships are used to calculate the price of produced water [21-23]:

$$CRF = \frac{i(1+i)^n}{(1+i)^n - 1}$$
 (13)

CRF is the capital recovery coefficient, i is the interest rate of lending banks (20% in Iran), and n is the system's life (10 years). The first annual cost of the system is calculated as follows:

$$FAC = P \times crf \tag{14}$$

P is the initial capital. The first annual return on capital (ASV) is calculated from the following equation:

$$ASV = Z \times SSF \tag{15}$$

Z is the rate of return on capital, and is usually taken as 20% of the cost of consumables (Z = 0.2P). SSF is the non-returnable capital factor, and is calculated as follows:

$$SSF = \frac{i}{(1+i)^n - 1}$$
 (16)

The annual maintenance cost of the system is calculated from the following equation:

$$AMC = 0.15 \times FAC \tag{17}$$

The total annual cost of the system is calculated as follows:

$$AC = FAC + AMC - ASV$$
 (18)

Finally, the cost of each liter is calculated as follows:

$$CPL = \frac{AC}{M} \tag{19}$$

M is the annual productivity of distilled fresh water that calculated for 365 days of a year and the system operate on average 10 hours for each day. The annual cost of water production according to equations (13) to (19) was obtained based on the use of solar energy in the system. The annual energy consumption cost in equation (17) is considered, and since the assumption was made to use solar energy, it was considered free. It should be noted that a series of experiments were performed on a solar air heater during the summer season, and based on that, an electric air heater was built.

4. Results and discussion

This experimental study proposes a solar HDH desalination system as an open-air-open water type. A new condenser (OAOW) thermoelectric modules is used to dehumidify the dehumidifier unit. The effect of the two parameters of the inlet temperature on the humidifier tower and the airflow rate of the inlet to the system has been investigated, to evaluate the system performance, efficiency, GOR, COP, and condenser efficiency have been calculated and checked. Economic analysis is also presented in the proposed model. Also it could be important to mentione that the inlet air temperature to the condenser is one of the parameters that cannot be controlled and depends on the path that the air

travels during the process. Only the flow rate and the inlet air temperature were controllable during the experiment. On the other hand, the electric heater was also made up of five elements for heating, and by turning on each element, the inlet air temperature reached a specific temperature.

4.1. Fresh water production

Fresh water production was evaluated in three different air flow rates and by changing the inlet air temperature in four stages. Figure 4 shows that as the inlet air temperature increases from 49 to degrees Celsius, freshwater production increases in all three air flow rates. It can be said: "As the temperature of the incoming air increases, the humidity of the air growths, and more humidity enters the condenser per kilogram of dry air; also at high temperatures, evaporation takes place at a higher rate." On the other hand, an increase in air temperature causes an increase in the dew point temperature of the available humidity, as a result of which the difference with the surface temperature of the heat sinks inside the condenser increases, and ultimately desalination rate rises. The main point of the graph is that the amount of water produced is close to each other in two airflow rates of 0.022 and 0.027 kg/s for temperatures less than 69 degrees Celsius. To ensure the precision of the experimental data, the error value was calculated according to equation (12) for all test conditions, the maximum value of error was 10%. To ensure condensation inside the condenser, heat transfer must be done effectively. Two parameters are important for heat transfer: the time for heat exchange and the temperature difference between the air and the heat sink surface. At a flow rate of 0.027 kg/s at low temperatures, the temperature difference between the air and the heat sink is low and the air velocity is high, resulting in poor heat exchange. As the inlet air temperature increases, the temperature difference between the air and the heat sink increases, and it overcomes the air velocity.

To perform condensation, humid air has enough time for heat exchange inside the condenser or there is a large temperature difference between the humid air and the surface of the heatsinks. According to figure 4, at the inlet air flow rate equal to 0.027 and 0.022, the water production rate at temperatures below 69 degrees Celsius are so close to each other; because at an air flowrate equal to 0.027 kg/s, the air moves through the condenser quickly and do not have enough opportunity for heat exchange with cool heatsinks. The reason for the impressive increase in the

water production rate after the temperature of 69 degrees Celsius is that the temperature difference of the air passing through the condenser with the surface temperature of the heatsinks is superior to the speed of the airflow passing through the condenser.

Figure 5 shows the freshwater produced at constant temperature for three different inlet air flow rates. Based on the experimental results, it can be concluded that at low temperatures (65-49) degrees Celsius, due to the approach of the air to the saturation state, the extremum point occurs at a flow rate of 0.022 kg/s. At high temperatures (75-85 degrees Celsius), the vapour-carrying capacity of dry air increases. Increasing the airflow in the test range does not saturate the air, and the graph rises linearly. At higher flow rates, the extreme point will also occur for temperatures of 75 and 85 degrees Celsius.

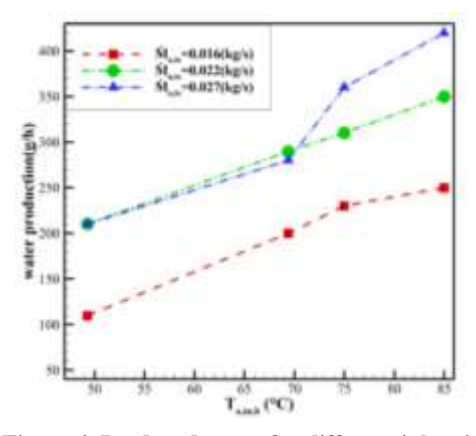


Figure 4. Produced water for different inlet air temperatures by flow rate.

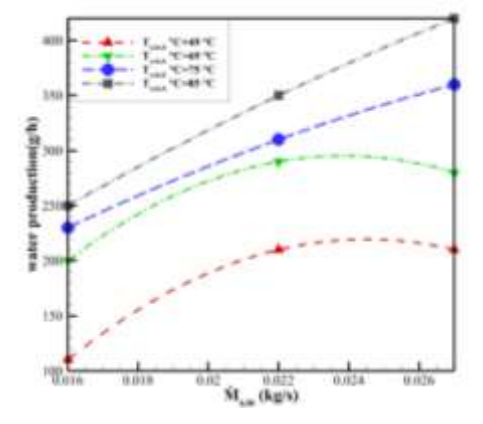


Figure 5. Produced water for different flow rates by different inlet air temperatures.

4.2. Condenser efficiency

According to figures 6 and 7, the efficiency of the condenser is only dependent on the temperature, and the flow rate of the incoming air does not affect the efficiency of the condenser. The reason for this can be explained as follows: due to the increase in heat input to the condenser and the

constant power of the thermoelectric, the efficiency first increases until it reaches the maximum power of the thermoelectric. After a specific temperature, the increase in thermal load will have a negative effect on the performance of thermoelectric, and their efficiency will decrease; As a result, the graph takes a decreasing trend. From the diagram in figure 6, we can conclude that the maximum efficiency of the condenser occurs at a temperature of 69 degrees Celsius.

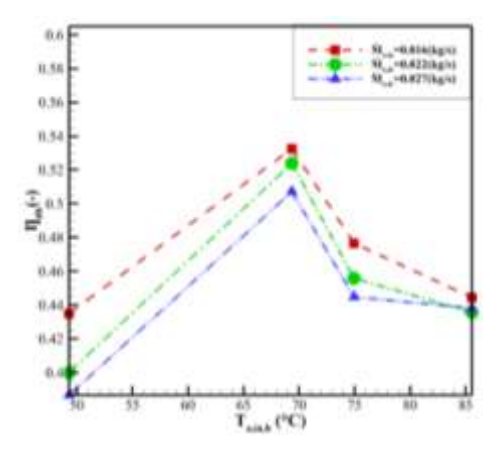


Figure 6. Dehumidifier efficiency according to the temperature of the air entering the system.

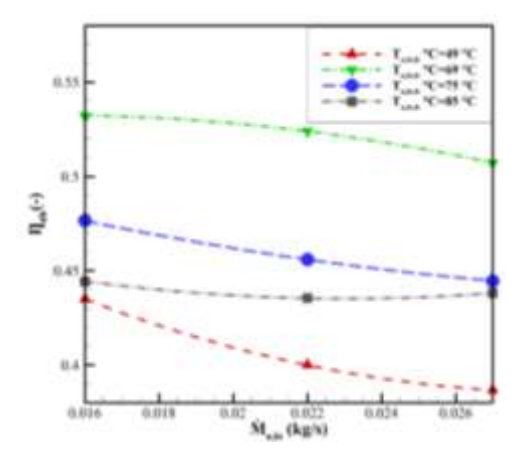


Figure 7. Dehumidifier efficiency in terms of air flow rate entering the system.

The coefficient of performance of the condenser (COP) is obtained from the ratio of the thermal power (cooling) taken from the humid air entering the condenser to the input electrical power (sum of the electrical power consumed by the thermoelectric and the pump). According to figure 8, at a constant flow rate, the COP increases with the increase of the temperature of the air entering the system. Due to the constant power consumption of thermoelectric and the constant flow of cooling water, the cooling load in the condenser remains constant; on the other hand, increasing the temperature of the air entering the condenser increases the temperature difference between the surface of the heatsinks and the

temperature of the humid air; as a result, more moisture condenses, and finally, the performance coefficient of the condenser increases.

At low temperatures (49-69 degrees Celsius), increasing the flow rate of the air entering the system increases the COP, and after the flow rate reaches 0.022 kg/s, the COP is almost constant. But at high temperatures (75-85 degrees Celsius) the COP changes with the intake air flow rate are almost linear. It is also expected that the extremum point will occur at higher flow rates at high temperatures. By increasing the flow rate of the incoming air, it can be expected that the amount of water produced and the COP of the condenser will increase as more water molecules collide with the surface of the cool heat sinks. In this study, the highest COP equal to 0.78 was obtained, corresponding to the incoming air's temperature and flow rate of 85.6 degrees Celsius and 0.027 kg/s.

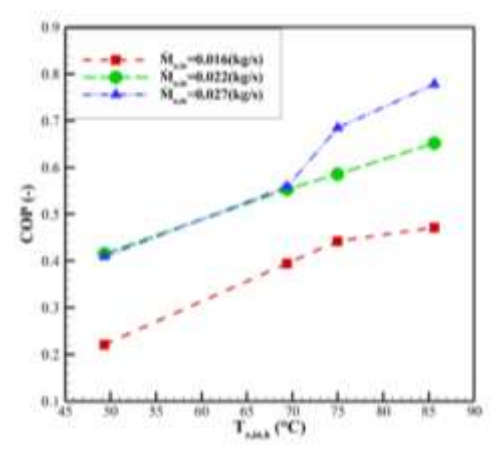


Figure 8. Condenser COP at different temperatures at a given flow rate.

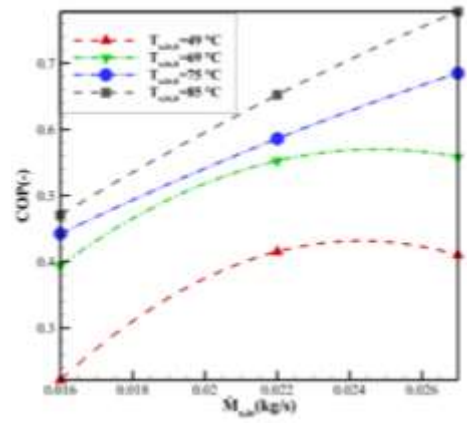


Figure 9. Condenser COP at different inlet air flow rates by temperature.

4.4. Changes in humidity ratio of inlet and outlet air of condenser

Another important parameter to check the performance of the condenser is the changes in the humidity ratio of the incoming and outgoing air

from the condenser. Figures 10 and 11 show that the air humidity ratio at a constant flow rate increases with the inlet air temperature entering the system, both at the inlet and outlet of the condenser. Similarly, it can be observed that at an airflow rate equal to 0.016 kg/s, due to the closeness of the air to the saturation state, at temperatures higher than 75 degrees Celsius, the humidity ratio is almost constant. The changes in the air humidity ratio at the inlet and outlet of the condenser, at an airflow rate of 0.022 kg/s, is almost a linear function of temperature. However, it is expected that the air will reach saturation at higher temperatures and the humidity ratio will be fixed. At a flow rate of 0.027 kg/s, at temperatures below 69 degrees Celsius, air enthalpy is low, and due to the high speed of the air passing through the humidifier tower, air with a lower humidity ratio enters the condenser; but as the temperature increases and the enthalpy increases, the incoming air can carry a larger volume of small water particles; as a result, the humidity ratio increases.

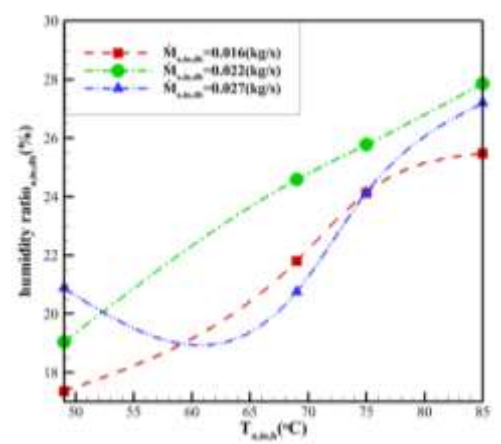


Figure 10. Humidity ratio of the air entering the condenser for different temperatures of the air entering the system.

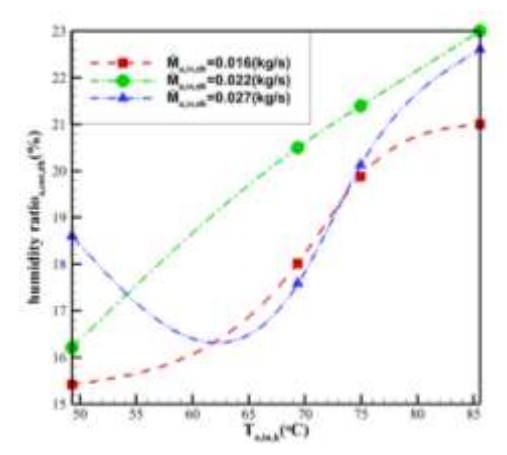


Figure 11. Humidity ratio of the air leaving the condenser for different temperatures of the air entering the system.

On the other hand, figures 12 and 13 show that at a temperature of 49 degrees Celsius, increasing

the flow rate causes an increase in the humidity ratio at both the inlet and outlet of the condenser; but at temperatures higher than 69 degrees Celsius, the trend of changing the humidity ratio with the flow rate of the incoming air is parabolic with a negative slope, the maximum of which occurs at the flow rate of 0.022 kg/s. At a temperature of 49 degrees Celsius, with the increase of the incoming air flow rate, more evaporation takes place, and the humidity ratio increases. The reason for the existence of the maximum point at temperatures higher than 69 degrees Celsius is that the air reaches its final capacity to accept and carry water molecules according to the conditions of the system.

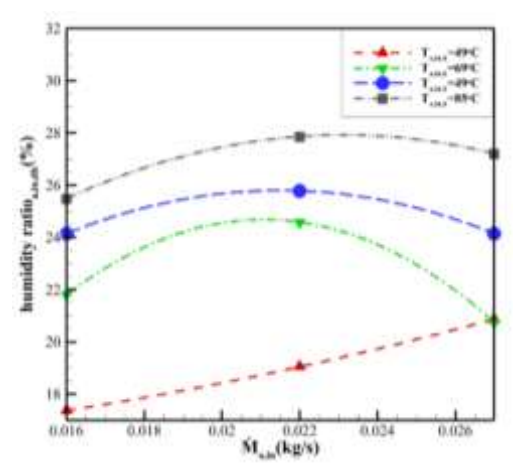


Figure 12. Humidity ratio of the incoming air to the condenser for different flow rates of the incoming air to the system.

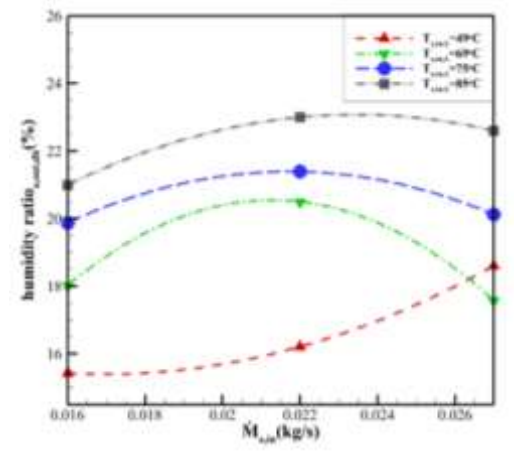


Figure 13. Humidity ratio of the air leaving the condenser for different flow rates of the air entering the system.

The difference in air humidity ratio at the inlet and outlet of the condenser was also checked according to the temperature and flow rate of the air entering the system (Figures 14 and 15). According to figure 14, the difference between the humidity ratio at the inlet and outlet of the condenser, at the flow rates of 0.016 and 0.027 kg/s, increases with the increase in the

temperature of the air entering the system, and the slope of the graph will decrease from the temperature of 75 degrees Celsius; but at a flow rate of 0.022 kg/s, the graph is almost linear. Figure 15 also shows that the graph of the difference between the humidity ratio at the inlet and outlet of the condenser at a constant temperature, with the increase in flow rate, is parabolic and has a negative slope at all temperatures. According to figure 14, because the cooling load inside the condenser is constant, as the temperature of the inlet air to the condenser increases, the temperature difference between the inlet air and the surface of the heat sinks also increases, which leads to more condensation of the steam in the air; as a result, the difference in humidity ratio at the inlet and outlet of the condenser increases. As it can be seen in figure 15, at a flow rate of 0.022 kg/s, the air passes through the condenser at an optimal speed and has enough time for heat exchange. For this reason, the difference in humidity is greater in this flow rate.

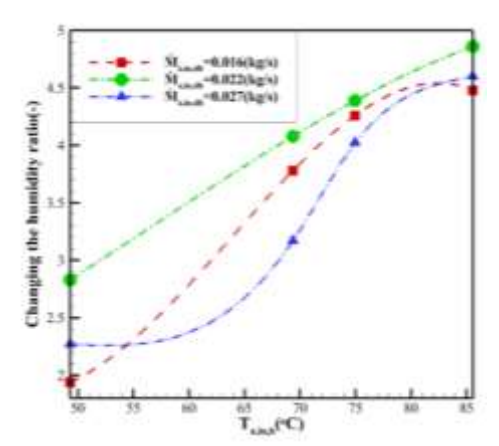


Figure 14. Change of the humidity ratio of inlet and outlet air for different temperatures.

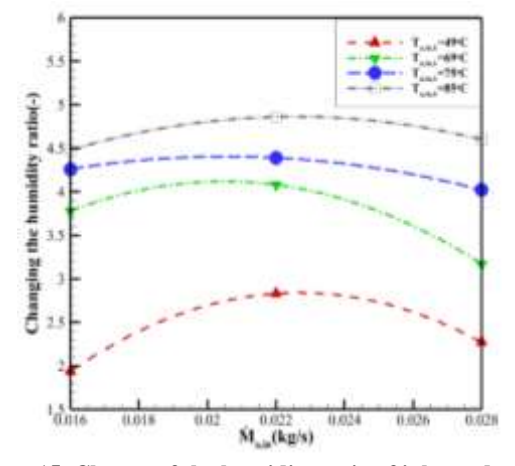


Figure 15. Change of the humidity ratio of inlet and outlet air for different flow rates.

4.5. GOR

The rate of GOR change has an inverse relationship with the total heat input to the system, and a direct relationship with the amount of freshwater produced. It is worth noting that the increase in heat input will have a negative effect and the increase in freshwater production will positively affect the GOR rate. Figure 16 shows the effect of these two parameters. As it can be seen, in the investigation of the effect of increasing the temperature of the inlet air (to the humidifier tower) on the GOR, at the air inlet flow rate equal to 0.016 kg/s with the temperature increase from 49 to 75 degrees Celsius, the GOR has an upward trend, and after that as the temperature increases to 85 degrees Celsius, its value decreases; because even though in this experiment, the amount of water production increases with the increase in temperature (Figure 8), but the amount of heat input to the system will also increase with the increase in temperature, and the effect of increasing the heat input to the system will be greater at temperatures above 75 degrees Celsius; as a result, the GOR value decreases. GOR at the inlet air flow rate higher than 0.016 kg/s decreases with increasing temperature and remains almost constant after that. As mentioned earlier, the negative effect of the inlet air flow rate of 0.027 kg/s for water production and its effect on GOR is also evident (Figure 16). In such a way that the graph related to the airflow rate of 0.027 kg/s, at temperatures less than 69 degrees Celsius, is lower than the airflow rate graph of 0.022 kg/s; because due to the high speed of the airflow, good heat exchange does not take place inside the condenser, and the air that has exergy easily leaves the system.

If a constant temperature difference between the inlet and outlet of the electric air heater is required, the heat required for air heating increases with the increase of the airflow rate. This event in the solar air heater can be explained in this way the intensity of the sun's radiation increases during certain hours of the day, so the airflow should be adjusted accordingly so that the output temperature of the solar heater is at the highest value. In this situation, increasing the flow rate of the incoming air causes an increase in the heat input to the system and also causes an increase in the production of fresh water. According to equation (10), the airflow rate increase has a direct relationship with the GOR rate, while the increase in input heat will have an inverse relationship with the GOR rate. Finally, in the effective results of these two parameters, according to figure 17, GOR shows a parabolic behavior with the increase of flow rate at temperatures lower than 69 degrees Celsius, its maximum point occurs at the flow rate of 0.022 kg/s. At temperatures above 75 °C, GOR increases linearly with a very low slope.

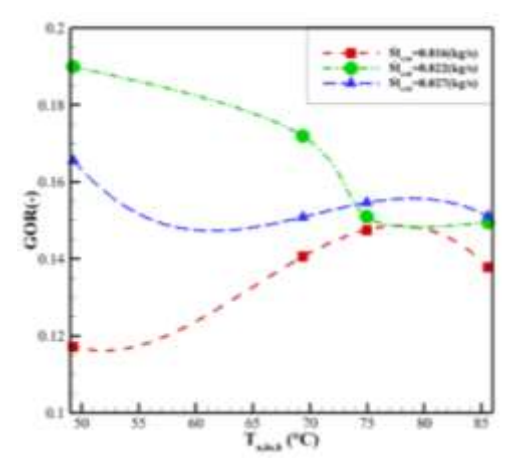


Figure 16. Thermal efficiency of the system for different inlet air temperatures by air flow rate.

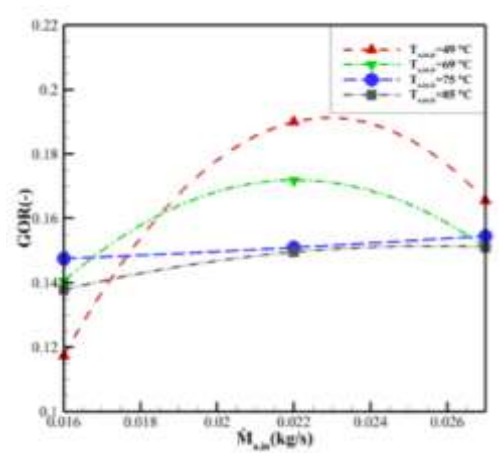


Figure 17. Changes in the GOR of the system for different flow rates by air temperature.

4.6. Economic analysis

Tables 6 and 7 show the proposed construction cost and economic analysis results. The amount of annual water production and the cost of produced water in the best conditions are estimated as 1533 liters per square meter and 0.049 dollars per liter per square meter, respectively, based on the test results.

Table 6. System construction costs.

Components	Price \$	Recycling cost \$
Solar air heater	50	10
Fan	13	5
Humidifier tower	55	20
Thermoelectric	30	-
Pump	20	10
Other components (pipes, ducts, Connections,)	10	-
Power supply	70	30
Heat sinks	34	5

Table 7. Results of economic analysis of the system

I	CRF	fac	ASV	S	SSF	AMC	Ac	CPL
0.2	0.24	67.26	2.17	56.4	0.038	10.09	75.18	0.098- 0.049

Considering that the highest GOR of the system is related to the flow rate of the incoming air equal to 0.022 kg/s and the temperature of the incoming air equal to 46.6 degrees Celsius, the cost of water production will be equal to 0.098 dollars. On the other hand, at the inlet airflow rate of 0.027 kg/s and the inlet air temperature at 83.6 degrees Celsius, the highest COP and the highest amount of produced water have been obtained. In this case, the cost of produced water will be 0.049 dollars. In Table 8, a comparison of the present study with some studies of the recent years can be made. The studied system has the ability to produce considerable water.

5. Conclusion

This study presented a new HDH water desalination system design with a thermoelectric Considering reference condenser. [8], of OAOW importance systems has been emphasized. On the other hand, since incoming water is used for cooling thermoelectricity in the system, its temperature increases, and it cannot complete the closed cycle. The presented model of the HDH desalination system combined with the thermoelectric condenser has been introduced as a novel structure for recovering systems waste heat, and then the experimental tests done. The results section presents the system's performance in the form of freshwater production rate, thermoelectric condenser performance coefficient, GOR rate, and economic analysis. All experiments conducted in Babol, Iran (latitude: 36.54° N, longitude: 52.68° E, and altitude: -2 m above sea level) between 8:00 AM and 5:00 PM in March 2022, and the effect of Two parameters of temperature and inlet air flow have been investigated on the performance of the system. The important results of this study are as follows:

- The designed system is very cheap and its maintenance costs are very low; also it is simple in terms of fluid circulation.
- In this research work, the flow of salt water entering the system has been used to cool the thermoelectrics, which causes the absorption of the heat emitted from the condenser chamber by the water, and the incoming water is preheated and evaporation takes place better.
- Increasing the temperature of the air entering the system at a specific flow rate

- increases the amount of water produced. In addition, the results showed that more water would be produced by increasing the flow rate of the incoming air.
- (COP) of the condenser increases due to the constancy of the power consumption of the thermoelectric and the pump with the increase of both temperature parameters and the inlet airflow rate.
- The lowest COP value of the system is obtained at a flow rate of 0.016 kg/s and an inlet air temperature of 49 degrees Celsius, equal to 0.22.
 - Also The highest value of COP is obtained at the flow rate of 0.027 kg/s and the inlet air temperature is 85 degrees Celsius, equal to 0.78.
- The GOR of the system has an inverse relationship with the amount of energy input to the system. The amount of input energy also depends on the two parameters of air flow rate and heat given to the air. During the experiment, the amount of heat given to the incoming air is much higher than the rate of increase in water production at the inlet air flow rate equal to 0.022 and 0.027 kg/s. For this reason, the graph takes a decreasing trend.
- At low temperatures, the trend of GOR changes with the increase of inlet air flow rate is a parabolic diagram, the maximum point of which occurs in the ratio of water production to maximum input energy.

- GOR increases linearly and with a very low slope at higher temperatures compared to the inlet flow rate. The highest value of GOR was also obtained at a flow rate of 0.022 kg/s and an inlet air temperature of 47.5 degrees Celsius and equal to 0.19.
- In this system, the cost of producing each liter of fresh water per year is in the range of 0.098-0.049 dollars, which is very suitable, compared to other introduced water desalination systems of this model.
- Investigations have shown that using HDH water desalination systems is highly efficient in places where brine water is available. Because at these points, it is possible to increase the flow rate of the condenser cooling water by keeping the electric energy consumption constant and improving the system's efficiency.
- This built condenser can be placed in conditions with humid air that does not require a humidifying tower and an air heater. Also, thermoelectric can be used to cool the water in a tank, and cold water can be used to flow inside finned tubes as condenser. In this case, water can be produced throughout the day and night.

For future work, it could be a good suggestion to model the system numerically in order to improve the performance by determining systems low performance components.

CPL	GOR	Type of cooling system	Type of energy used	Fresh water production	Year of construction	Reference
0.1055	-	Thermoelectric	Solar-urban electricity	1033 (L/m².year)	2020	Shoeibi et al. [24]
0.03	1.93	Vapor compression refrigeration	Solar-urban electricity	17.45 (kg/h)	2019	Zhao et al. [25]
0.097	-	Thermoelectric	Solar-urban electricity	711 (L/m².year)	2020	Omedi <i>et al</i> . [15]
0.0204-0.016	4.07	-	Solar	12 (L/h)	2020	Khalifa et al. [26]
0.0252	-	Thermoelectric	Solar-urban electricity	1689 (L/m².year)	2018	Nazari <i>et al</i> . [16]
0.1422	-	Thermoelectric	Solar-urban electricity	912 (L/m².year)	2017	Rahbar et al. [27]
0.049-0.098	0.19	Thermoelectric	Solar-urban electricity	420 (mL/h)	2022	current study

Table 8. Comparison of the present study with some studies of recent years.

6. Nomenclature

m	Inlet dry air mass
m _a	Specific heat capacity of air (kj/kg-K)
Cpair	Dry air flow (kg/s)
aṁ	
T ₀	Environment air temperature (°C)
T ₁	Humidifier inlet air temperature (°C)
T ₂	Condenser inlet air temperature (°C)
T ₃	Condenser outlet air temperature (°C)
h_{fg}	Mixture of water and saturated steam Enthalpy (kj/kg)
fm	Experimentally produced water (kg/s)
_{ff} ṁ	Theoretically produced water (kg/s)
V_{air}	Inlet air speed (m/s)
i	Bank interest rate
X	Average value of the data
U_c	Combined uncertainty
$T_{i,h}$	Air temperature at humedifire inlet (°C)
$\eta_{ m DH}$	Condenser efficiency
$\omega_{o,\mathrm{dh}}$	Absolute humidity at dehumedifire outlet (kg/kg)
Z	Rate of return on capital
M	annual productivity of distilled fresh water
h_{f2}	Enthalpy of saturated water at temperature T ₂ (kj/kg)
h_{f3}	Enthalpy of saturated water at temperature T ₃ (kj/kg)
2ω	Humidity ratio at temperature T ₂ (kg/kg)
3ω	Humidity ratio at temperature T ₃ (kg/kg)
Et	Total electrical energy (W)
E _{th}	Electric energy consumed by thermoelectrics (W)
Ep	Electric energy consumption of pump and blower (W)
Qcollector	Heat absorbed by collector (W)
Q _{tot}	Total heat supplied to the system (W)
A	Inlet cross-section
ρ	Air density
n	System lifetime
S	Standard deviation
k	Coverage factor
T_{∞}	Ambient air temperature (°C)
$\omega_{i,dh}$	Absolute humidity at dehumidifier inlet (kg/kg)
	Absolute humidity related to the air leaving the
$\omega_{o,dh,s}$	dehumidifier in saturated state (kg/kg)
P	Initial capital

7. Abbreviations

COP	Coefficient of performance of the condenser
GOR	Gain of Ratio of the system
CRF	Capital recovery coefficient
FAC	First annual cost of the system
ASV	First annual return on capital
SSF	Non-returnable capital factor
AMC	Annual maintenance cost of the system
AC	Total annual cost of the system
CPL	Cost of each liter

8. References

- [1] D. Lawal, M. Antar, A. Khalifa, S. Zubair, and F. Al-Sulaiman, "Humidification-dehumidification desalination system operated by a heat pump," Energy Conversion and Management, Vol. 161, pp. 128-140, 2018.
- [2] A. Mohamed, M. S. Ahmed, H. M. Maghrabie, and A. G. Shahdy, "Desalination process using humidification—dehumidification technique: A detailed review," International Journal of Energy Research, Vol. 45, pp. 3698-3749, 2021.
- [3] Y. Ghalavand, M. S. Hatamipour, and A. Rahimi, "A review on energy consumption of desalination

- processes," Desalination and Water Treatment, Vol. 54, pp. 1526-1541, 2015.
- [4] E. Deniz and S. Çınar, "Energy, exergy, economic and environmental (4E) analysis of a solar desalination system with humidification-dehumidification," Energy Conversion and Management, Vol. 126, pp. 12-19, 2016.
- [5] T. Alam and M.-H. Kim, "Performance improvement of double-pass solar air heater—A state of art of review," Renewable and Sustainable Energy Reviews, Vol. 79, pp. 779-793, 2017.
- [6] D. U. Lawal and N. A. Qasem, "Humidification-dehumidification desalination systems driven by thermal-based renewable and low-grade energy sources: A critical review," Renewable and Sustainable Energy Reviews, Vol. 125, p. 109817, 2020.
- [7] M. Faegh, P. Behnam, and M. B. Shafii, "A review on recent advances in humidification-dehumidification (HDH) desalination systems integrated with refrigeration, power and desalination technologies," Energy Conversion and Management, Vol. 196, pp. 1002-1036, 2019.
- [8] K. H. Mistry and A. Mitsos, "Optimal operating conditions and configurations for humidification—dehumidification desalination cycles," International Journal of Thermal Sciences, Vol. 50, pp. 779-789, 2011.
- [9] M. H. Sharqawy, M. A. Antar, S. M. Zubair, and A. M. Elbashir, "Optimum thermal design of humidification dehumidification desalination systems," Desalination, Vol. 349, pp. 10-21, 2014.
- [10] R. Santosh, G. Kumaresan, G. K. Kumar, and R. Velraj, "Experimental parametric investigation of waste heat powered humidification dehumidification system for production of freshwater from wastewater," Desalination, Vol. 484, p. 114422, 2020.
- [11] Y. Elhenawy, M. Abd Elkader, and G. H. Moustafa, "A theoretical model for a humidification dehumidification (HD) solar desalination unit," International Journal of Energy and Power Engineering, Vol. 9, pp. 646-655, 2015.
- [12] M. Siahmargoi, N. Rahbar, H. Kargarsharifabad, S. E. Sadati, and A. Asadi, "An experimental study on the performance evaluation and thermodynamic modeling of a thermoelectric cooler combined with two heatsinks," Scientific Reports, Vol. 9, pp. 1-11, 2019.
- [13] J. Vián, D. Astrain, and M. Dominguez, "Numerical modelling and a design of a thermoelectric dehumidifier," Applied Thermal Engineering, Vol. 22, pp. 407-422, 2002.
- [14] Y. Yao, Y. Sun, D. Sun, C. Sang, M. Sun, L. Shen, et al., "Optimization design and experimental study of thermoelectric dehumidifier," Applied Thermal Engineering, Vol. 123, pp. 820-829, 2017.
- [15] B. Omidi, N. Rahbar, H. Kargarsharifabad, and S. Rashidi, "Combination of a solar collector and

- thermoelectric cooling modules in a humidification—dehumidification desalination system-experimental investigation with energy, exergy, exergoeconomic and environmental analysis," Energy Conversion and Management, Vol. 225, p. 113440, 2020.
- [16] S. Nazari, H. Safarzadeh, and M. Bahiraei, "Performance improvement of a single slope solar still by employing thermoelectric cooling channel and copper oxide nanofluid: an experimental study," Journal of cleaner production, Vol. 208, pp. 1041-1052, 2019.
- [17] B. Alizadeh Kharkeshi, R. Shafaghat, R. Alamian, and A. H. Aghajani Afghan, "Experimental & Analytical Hydrodynamic Behavior Investigation of an Onshore OWC-WEC Imposed to Caspian Sea Wave Conditions," International Journal of Maritime Technology, Vol. 14, pp. 1-12, 2020.
- [18] H. Panchal, K. K. Sadasivuni, C. Prajapati, M. Khalid, F. Essa, S. Shanmugan, et al., "Productivity enhancement of solar still with thermoelectric modules from groundwater to produce potable water: a review," Groundwater for Sustainable Development, Vol. 11, p. 100429, 2020.
- [19] R. Shafaghat, M. Fallahi, B. Alizadeh Kharkeshi, and M. Yousefifard, "Experimental Evaluation of the Effect of Incident Wave Frequency on the Performance of a Dual-chamber Oscillating Water Columns Considering Resonance Phenomenon Occurrence," Iranian (Iranica) Journal of Energy & Environment, Vol. 13, pp. 98-110, 2022.
- [20] B. Alizadeh Kharkeshi, R. Shafaghat, O. Jahanian, R. Alamian, and K. Rezanejad, "Experimental study on the performance of an oscillating water column by considering the interaction effects of optimal installation depth and dimensionless hydrodynamic coefficients for the Caspian Sea waves

- characteristics," Ocean Engineering, Vol. 256, p. 111513, 2022/07/15/2022.
- [21] A. E. Kabeel, A. Hamed, and S. El-Agouz, "Cost analysis of different solar still configurations," Energy, Vol. 35, pp. 2901-2908, 2010.
- [22] H. E. Fath, M. El-Samanoudy, K. Fahmy, and A. Hassabou, "Thermal-economic analysis and comparison between pyramid-shaped and single-slope solar still configurations," Desalination, Vol. 159, pp. 69-79, 2003.
- [23] S. Kumar and G. Tiwari, "Life cycle cost analysis of single slope hybrid (PV/T) active solar still," Applied energy, Vol. 86, pp. 1995-2004, 2009.
- [24] S. Shoeibi, N. Rahbar, A. A. Esfahlani, and H. Kargarsharifabad, "Application of simultaneous thermoelectric cooling and heating to improve the performance of a solar still: an experimental study and exergy analysis," Applied energy, Vol. 263, p. 114581, 2020.
- [25] H. Xu, Y. Zhao, and Y. Dai, "Experimental study on a solar assisted heat pump desalination unit with internal heat recovery based on humidification-dehumidification process," Desalination, Vol. 452, pp. 247-257, 2019.
- [26] D. U. Lawal, M. A. Antar, A. Khalifa, and S. M. Zubair, "Heat pump operated humidification-dehumidification desalination system with option of energy recovery," Separation Science and Technology, Vol. 55, pp. 3467-3486, 2020.
- [27] N. Rahbar, A. Gharaiian, and S. Rashidi, "Exergy and economic analysis for a double slope solar still equipped by thermoelectric heating modules-an experimental investigation," Desalination, Vol. 420, pp. 106-113, 2017.